A stabilized hybrid FE/FV method applied to fluid flow in mold filling

Jürgen Neises* — Gottfried Laschet**

**Fujitsu Siemens Computers*
Gladbecker Str. 7
40472 Düsseldorf, Germany
juergen.neises@fujitsu-siemens.com

***ACCESS e.V.*
Intzestr. 5, 52072 Aachen
Germany
g.laschet@access.rwth-aachen,de

ABSTRACT. *Modern casting processes allow the precise production of parts with complex shapes. Numerical simulation increasingly becomes an important tool aiding design and production. A finite element method using finite volume principles is described. A new adaptive stabilization based either on bubble functions or a Petrov-Galerkin method is elaborated. Then, a new stabilization scheme, named FF-VOF, is presented to describe the free surface evolution during mold filling. Finally, the developed method is applied to the mold filling benchmark defined at the 7th Conference on Modeling of Casting, Welding and Advanced Solidification Processes.*

RÉSUMÉ. *Les procédés modernes de fonderie permettent la production précise de pièces à géométries complexes. La simulation numérique y devient de plus en plus un outil important d'aide à la conception et à la production des pièces coulées en fonderie. Une formulation basée sur la méthode des éléments finis mais utilisant aussi des principes volumes finis est introduite pour simuler l'écoulement du métal liquide. Une nouvelle technique de stabilisation basée soit sur les modes bulles soit sur la méthode de Petrov-Galerkin est élaborée. Puis, un nouveau schéma de stabilisation est présenté pour décrire l'évolution de la surface libre durant le remplissage du moule. Finalement, cette méthode est validée par la prédiction du remplissage du benchmark proposé à la 7e conférence MCWASP.*

KEYWORDS: *casting processes, incompressible flow, pressure stabilization, finite volumes, stabilized finite element methods, MINI element.*

MOTS-CLÉS : *procédés de fonderie, écoulement incompressible, pression stabilisée, méthode d'éléments finis stabilisés, élément MINI.*

1. Introduction

Modern casting processes allow the precise production of parts with complex shapes. Thus, casting is a widely used industrial process technology. Concerning the manufacturing of complex industrial parts with high quality even in small series, a reliable and predictive numerical simulation increasingly becomes an inevitable part of the production chain (Haldenwanger, Stich, 2000, Sahm, Hansen, 2000). The physics, which are involved in casting and solidification processes, are tightly coupled. Hence, an integrated simulation tool is absolutely necessary to deliver a qualified analysis of casting processes (Dhatt, Gao, Ben Cheikh 1990, Song, Dhatt, Ben Cheikh, 1990).

CASTS, which is developed at ACCESS and at the foundry institute of Aachen University since the late eighties, is such an integrated tool to simulate 3D solidification problems. Currently it covers heat transfer including radiation heating, stress/strain analysis and free surface flow (Figure 1). In this paper the approach developed to model the melt flow is presented. A comprehensive overview of models and applications of CASTS to casting processes has been published in (Laschet, Neises, Steinbach, 1998a, Laschet, Neises, Diemer, 1998b).

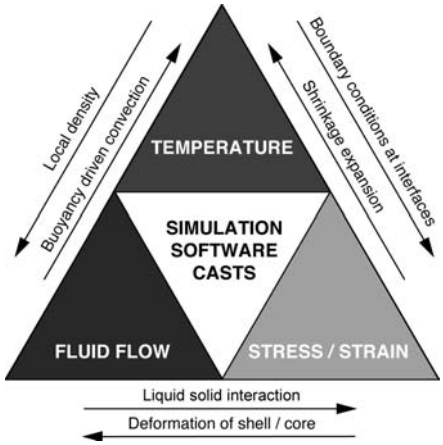

Figure 1. *The coupling of physics in CASTS for the casting process modeling. Combined 3-D heat and fluid flow can be evaluated including radiosity and free surfaces. The thermomechanical coupling allows to model contact or air gap formation between mould and metal*

CASTS is based on FE approximations of the discretized fields (velocity, pressure, temperature, etc.). Recently a hybrid approach was developed to combine the geometrical and mathematical features of the FE method with the computational simplicity of the FV method (Laschet, Neises, Steinbach, 1998a, Laschet, Neises,

Diemer, 1998b, Neises, Steinbach, 1996, Steinbach, Neises, 1995). By this means, all techniques used within the FE method can be applied. Furthermore, the main features of an FV method can be reproduced by constructing unstructured stencils. These arbitrary stencils are calculated at the start of the numerical simulation using the FE enmeshment. The hybrid FE/FV method works on virtual finite volumes resulting from the calculated stencils. There is no geometrical description of the cells. During the transient calculation matrix assembly is thus drastically simplified, since no further finite element integrations are realized.

As the density of liquid melt is almost constant, flow of the melt may be modeled as an incompressible fluid. Incompressible flow requires special attention to solve the continuity equation correctly (Arnold, Brezzi, Fortin, 1984, Dhatt, Gao, Ben Cheikh, 1990, Gresho, Sani, 1998, Soulaimani, Fortin, Quellet, Dhatt, Bertrand, 1987, Tezduyar, Mittal, Ray, Shih, 1992) and to preserve mass. In an earlier attempt fluid flow was simulated in CASTS using first order velocity and piecewise constant pressure approximations on the elements coupled with an artificial compressibility approach (Neises, Steinbach, 1996, Laschet, Neises, Steinbach, 1998a, Laschet, Neises, Diemer, 1998b). This is a stable approximation fulfilling the inf-sup condition (Gresho, Sani, 1998). Nevertheless, it was not feasible for the simulation of mold filling using coarse meshes (Neises, Laschet, 1998). Thus, the constraint to use locally, in thin parts, coarse meshes requires an improved resolution of flow in these domains. As effective pressure boundary conditions are required in thin walled domains, a continuous pressure discretization should be used there.

However the resulting use of quadratic velocity approximations leads to a drastic increase of degrees of freedom (DOF) and requires much more computational resources in terms of memory and CPU time. Hence, equal order methods are fairly attractive due to the minor degrees of freedom and necessary computational requirements. But equal order methods applied to incompressible flow require special treatment of pressure resolution to ensure a correct solution (Gresho, Sani, 1998). Within the framework of finite elements stabilized methods like Petrov-Galerkin methods, bubble functions and recently the variational multiscale method are known for stabilizing the numerical solution (Brezzi, Bristeau, Franca, Mallet, Roge, 1992, Brezzi, Franca, Hugues, Russo, 1996, Brezzi, Franca, Hughes, Russo, 1997, Franca, Frey, Hughes, 1992, Franca, Frey, 1992a, Franca, Russo, 1996, Franca, Nesliturk, Stynes, 1998, Hughes, 1995). All these stabilizing techniques are closely related. Using any type of stabilization, sub-mesh scales are resolved and results are introduced into the mesh scale system. This way, the fine scale degrees of freedom are coupled locally to the coarse scale ones.

The main objective of this work is the development and implementation of a reliable flow solver based on the FE/FV framework using coarse meshes to be applicable to industrial casting processes. The solution of the coupled thermal – mold filling problem is out of scope of this paper. The temperature field is presumed to be available or solved separately within sufficient accuracy to be used as input to determine temperature dependent thermo-physical data within each time step.

Henceforth, the incompressible Navier-Stokes equations are discretized using the hybrid FE/FV method. This way the velocity field and the pressure field are approximated equally by first order finite elements reducing thus the number of DOF. Based on the classical MINI element (Arnold, Brezzi, Fortin, 1984) with its bubble functions a new stabilization scheme is developed. This stabilization is obtained by approximate condensation of the bubble functions using the Galerkin form of the momentum and continuity equations. Hence bubble stencils are derived. The obtained stabilization terms are limited locally by conventional stabilization methods as upwinding or Petrov-Galerkin methods. The FE/FV method and its adaptive stabilization are described within the following chapters. Then the capabilities of this new method are demonstrated on typical melt flow problems.

2. The Hybrid FE/FV-Method

2.1. *Motivation*

The finite volume (FV) method, evolved during the early seventies via the finite difference (FD) method. Today the FV method has many proponents in the field of fluid flow and heat transport simulation (Patankar, 1980). Several applications of FV method show this method to be attractive for the solution of advection dominant equations. On the other hand, the finite element (FE) method is a more general and consistent approach. It is very flexible in handling complex geometries and boundary conditions and is more accurate by using higher order shape functions. Its accuracy is proven for self-adjoint problems, *e.g*. heat conduction, stress strain analysis. The advantages of FE methods are plainly the disadvantages of FV method and vice-versa.

Therefore a new approach based on finite elements was developed at ACCESS some years ago (Steinbach, Neises, 1995, Neises, Steinbach, 1996). The objective was the development of a hybrid method combining the mathematical and geometrical flexibility of the FE method with a more physical interpretation of the FV method. To achieve these features a formal FV method based on a FE discretization with first order shape functions was developed and implemented in the FE code CASTS.

Idelsohn & Oñate (Idelsohn, Oñate, 1994) have shown that for the transient heat transfer equation the FV method and the FE method with linear shape functions and lumped masses result in equivalent discretizations. This fact is used to design the new hybrid FE/FV method for the melt flow by the discretization of the incompressible Navier-Stokes equations:

$$\begin{aligned} &\left(\rho\vec{u}\right)_t + \rho\left(\vec{u}\cdot\nabla\right)\vec{u} - \rho\upsilon\Delta\vec{u} + \nabla p = \rho\vec{g} \\ &\nabla\cdot\left(\rho\vec{u}\right) = 0 \end{aligned} \qquad [1]$$

2.2. *Discretization of the linearized Navier-Stokes equations*

Within the presented approach we will use a locally linearized Navier-Stokes equations only. At each element a mean velocity $\vec{v} = \bar{\vec{u}}$ is assumed. This approach is sufficient, if the velocity $\vec{u}$ does not vary much from one node to the other. Hence the linearized Navier Stokes equations are basis of our discretization method:

$$\begin{aligned} &(\rho\vec{u})_t + \rho(\vec{v}\cdot\nabla)\vec{u} - \rho\upsilon\Delta\vec{u} + \nabla p = \rho\vec{g} \\ &\nabla\cdot(\rho\vec{u}) = 0 \end{aligned} \qquad [1a]$$

At first, in order to solve this fluid flow problem, a Galerkin weak formulation of the linearized Navier-Stokes equations [1a] is realized:

$$\begin{aligned} &\sum_j \int\int_V \rho(\vec{u}_t)_j \Phi_j \Phi_i dVdt + \sum_j \int\int_V \rho\upsilon\,\vec{u}_j \nabla\Phi_j \nabla\Phi_i dVdt + \\ &\sum_j \int\int_V \rho\vec{v}\vec{u}_j \nabla\Phi_j \Phi_i dVdt + \sum_k \int\int_V p_k \nabla\Psi_k \Phi_i dVdt = \sum_j \int\int_V \rho\vec{g}\Phi_i dVdt \end{aligned} \qquad [2a]$$

$$\sum_j \int_V \rho\vec{u}_j \nabla\Phi_j \Phi_i dV = 0 \qquad [2b]$$

The thermo-physical data density ρ, kinematic viscosity ν vary there with the temperature. The local mean velocity $\vec{v}$ varies in time and is treated like thermo-physical data. The unknown fields (velocity $\vec{u}$ and pressure p) certainly vary in time. The velocity field is there approximated using linear shape functions, Φ_i, i=1,…, number of nodes; whereas the pressure field is approximated using Ψ_k, k=1,…, number of pressure variables. If an equal order approximation is adopted like in expressions [2], the same shape functions Φ_i are used to describe both unknown fields. Hence, i, j, k range from 1 to the number of nodes.

The key features of the new hybrid method are the reordering of the FE integrals attributed to the nodes in equations [2] and a finite-volume-like treatment of the thermo-physical data, which also may be interpreted as a local homogenization.

2.3. *Definition of virtual finite volumes on a finite element mesh*

Analogously to FV method unstructured stencils are constructed. Figure 2 shows schematically the definition of a stencil based on an unstructured FE mesh. At each node of the existing FE mesh a finite volume is defined without a real geometrical description of its boundaries. By mass lumping the mass is evaluated at the central node defining so the mass of the corresponding finite volume. The thermo-physical data are evaluated at the mid of the links, where cell faces may be assumed.

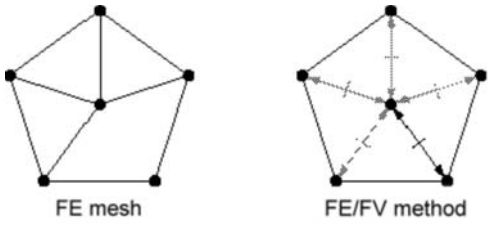

Figure 2. *Definition of an arbitrary stencil or virtual finite volume in a finite element mesh*

Similarly to FV or FD methods unstructured stencils are then constructed for the advective or diffusive operators. These stencils may be treated as in finite volume methods. Hence the implementation is simplified and the computing cost is decreased while preserving most of the approximation features of the FE method. Additionally, the optimal features of either method can be integrated, thus obtaining their benefits. (Idelsohn, Oñate, 1994, Zienkiewicz, Oñate 1991)

In hybrid FE/CV framework, there is always possible to define homogenized data $(\rho\upsilon)_{ij}, (\rho\vec{v})_{ij}$ at node i, where equations [3a, 3b] hold. These data are approximated in the common way of FV methods amidst the connecting link of nodes i and j:

$$\int_V \rho\upsilon \nabla\Phi_i \nabla\Phi_j dV = (\rho\upsilon)_{ij} \int_V \nabla\Phi_i \nabla\Phi_j dV, \qquad [3a]$$

$$\int_V \rho\vec{v} \nabla\Phi_j \Phi_i dV = (\rho\vec{v})_{ij} \int_V \nabla\Phi_j \Phi_i dV \qquad [3b]$$

$$\text{with } (\rho\upsilon)_{ij} = \tfrac{1}{2}\left((\rho\upsilon)_i + (\rho\upsilon)_j\right) (\rho\vec{v})_{ij} = \tfrac{1}{2}\left((\rho\vec{v})_i + (\rho\vec{v})_j\right) \qquad [3c]$$

To ensure the balancing principles of the FV method, the diagonal values $(\rho\upsilon)_{ii}, (\rho\vec{v})_{ii}$ have to be approximated properly. These values are defined canonically by:

$$(\rho\upsilon)_{\text{ii}} := -\frac{\sum_{j\neq i} (\rho\upsilon)_{\text{ij}} \int_V \nabla\Phi_i \nabla\Phi_j dV}{\int_V \nabla\Phi_i \nabla\Phi_i dV} \text{ and } (\rho\vec{v})_{\text{ii}} := -\frac{\sum_{j\neq i} (\rho\vec{v})_{\text{ij}} \int_V \Phi_i \nabla\Phi_j dV}{\int_V \Phi_i \nabla\Phi_i dV} \qquad [4]$$

These values need not to be calculated. They follow by summing the negative values of the off-diagonal terms to the diagonal of the discrete system. This is

analogous to classical FV methods and illustrates the balancing feature of the developed hybrid method.

Using equations [3] and [4] the thermo-physical data may be extracted from the integrals of the weak Galerkin formulation [2]. This way, the integration is separated into integrals over shape functions and integration in time as follows:

$$\sum_j \int \rho_{ij}(\vec{u}_t)_j dt \int_V \Phi_j \Phi_i dV + \sum_j \int (\rho \upsilon)_{ij} \vec{u}_j dt \int_V \nabla \Phi_j \nabla \Phi_i dV + \sum_j \int (\rho \vec{v})_{ij} \vec{u}_j dt \int_V \nabla \Phi_j \Phi_i dV + \sum_k \int p_k dt \int_V \nabla \Psi_k \Phi_i dV = \sum_j \int (\rho \vec{g})_{ij} dt \int_V \Phi_i dV \quad [5]$$

The extracted integrals of shape functions define arbitrary unstructured stencils for mass, diffusion or advection respectively, which can be calculated before the transient simulation starts. The term [6a] denotes the discrete gradient between volumes i and j. The term [6b] determines the discrete diffusion operator at the link of nodes i and j.

$$\int_V \nabla \Phi_j \Phi_i dV \quad [6a]$$

$$\int_V \nabla \Phi_j \nabla \Phi_i dV \quad [6b]$$

2.4. *Time integration of the momentum equation*

The temporal variation $(\rho \vec{u})_t$ in a time step can be discretized in several ways. A FV like discretization scheme is obtained by lumped masses. The time-integration of the discretized spatial operators, which are diffusion and advection, can be modeled by implementing conventional time-integration methods as θ-schemes:

$$\int_{t_n}^{t_{n+1}} f(t)dt = (1-\theta) f(t_n) + \theta f(t_{n+1}) = f(t_n) + \theta \left(f(t_{n+1}) - f(t_n) \right) \quad [7]$$

Within this scheme several well known one step methods are included. There are the explicit ($\theta = 0$) or implicit ($\theta = 1$) Euler scheme as well as the second order accurate implicit Crank-Nicholson scheme ($\theta = ½$). This 2nd order scheme is adopted here with $\theta = ½$.

First order shape functions, Φ_i are used to approximate the velocity and the pressure field. Gravity is interpreted as volumetric source term. Mass lumping is applied to the transient (mass) term as well as the source term. Additionally, the

advective term in the incompressible Navier-Stokes equation [1] is linearized. The linearization is applied locally and during each time step separately. Using the notation $\delta\vec{u} = \vec{u}(t_{n+1}) - \vec{u}(t_n)$, $\delta p = p(t_{n+1}) - p(t_n)$ and $\vec{u}^n = \vec{u}(t_n)$, $p^n = p(t_n)$, the Galerkin discretization of the Navier-Stokes [5] becomes:

$$\begin{aligned}
&\rho(\delta\vec{u})_i \int_V \Phi_i dV + \sum_{j\neq i} (\rho\vec{v})_{ij} \left[\left(\vec{u}_j^{\,n} - \vec{u}_i^{\,n}\right) + \theta\left(\delta\vec{u}_j - \delta\vec{u}_i\right)\right] \int_V \Phi_i \nabla\Phi_j dV \\
&+ \sum_{j\neq i} (\rho\upsilon)_{ij} \left[\left(\vec{u}_j^{\,n} - \vec{u}_i^{\,n}\right) + \theta\left(\delta\vec{u}_j - \delta\vec{u}_i\right)\right] \int_V \nabla\Phi_i \nabla\Phi_j dV \\
&+ \sum_{j\neq i} (\rho\vec{v})_{ij} \left[\left(p_j^n - p_i^n\right) + \theta\left(\delta p_j - \delta p_i\right)\right] = \rho_i \vec{g} \int_V \Phi_i dV, \text{ and} \\
&\sum_{j\neq i} \rho_{ij} \left[\left(\vec{u}_j^{\,n} - \vec{u}_i^{\,n}\right) + \theta\left(\delta\vec{u}_j - \delta\vec{u}_i\right)\right] \int_V \Phi_i \nabla\Phi_j dV = 0
\end{aligned} \qquad [8]$$

2.5. *Definition and resolution of the global system*

The global system of the flow problem is assembled in an analogous way as for FV methods. The hybrid approach reduces the element integrations to a single integration of shape functions and their gradients at the beginning of the transient analysis. These integrations require only few integration points, since the shape functions are of first order. Furthermore, for tetrahedrons exact analytic integration is possible. Additionally, matrix assembly consists only of combining the stencil and the averaged thermo-physical data. This task is easily implemented.

The FE/FV method works with less computational operations than required for the classical FE method. Whereas the FE method takes about 50 operations for a matrix entry, the hybrid FE/FV method requires only about 10 operations. Therefore the effort to assemble the global matrices at each time-step is reduced drastically.

After matrix assembly the boundary conditions have to be set. For the velocity either a slip or a no-slip condition can be imposed. The no-slip boundary condition is the more physical one, if the mesh size allows the solution of the boundary layer. Otherwise a slip condition allows the modeling of this boundary layer:

$$\begin{aligned}
&\vec{n} \cdot \vec{u} = 0 \\
&\vec{u}_t + \rho(\vec{v} \cdot \nabla)\vec{u} - \rho\upsilon\Delta\vec{u} + \nabla p = \rho\vec{g} - \gamma\vec{v}
\end{aligned} \qquad [9]$$

This way the flow is enforced to be tangential to the considered wall. The parameter γ generates a frictional force.

For the pressure, the normal gradient of the momentum equation [10] is selected as boundary condition within a closed domain on any boundary.

$$\vec{n} \cdot \nabla p = \vec{n} \cdot \nabla\left(\vec{u}_t + \rho\left(\vec{v} \cdot \nabla\right)\vec{u} + \rho\upsilon\Delta\vec{u}\right) \qquad [10]$$

At in-flow or out-flow boundaries only pressure boundary conditions are imposed as suggested by Gresho and Sani 1998. Even if, following them, the problem of proper out-flow conditions still is an delicate question in numerical flow simulation, the setting leads to a stable resolution of velocity and pressure at outflow boundaries. However, the development of a proper and consistent ouflow boundary condition is an important task in further development of CASTS.

3. The stabilized FE/FV-method

3.1. *Upwind schemes for the momentum equation*

The momentum equation can be seen as a system of advection-diffusion equations with ∇p acting as sink. Therefore the proper discretization of advective diffusive systems is also an important issue in modeling fluid flow. Either a sufficient fine adaptive enmeshment or a stabilization technique like an upwind scheme are required. Both approaches avoid oscillatory solutions. However, within the classical FE methods, either adaptive refinement or upwind techniques like SUPG (Brooks, Hughes 1982) are not straightforward to implement and are also costly in execution. But within the FV framework, upwind scheme are simple to implement (Patankar 1980). Therefore an upwind scheme analogous to FV methods has been adopted for advection-diffusion in the momentum equation [8]. Discrete advection and diffusion are there weighed up, thus reducing the effective local Reynolds number.

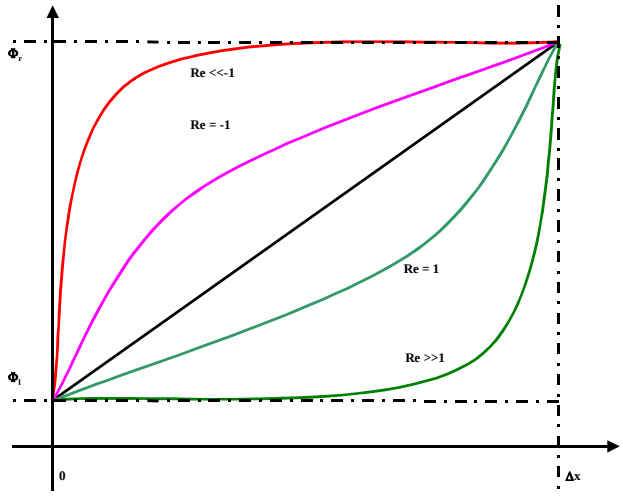

Figure 3. *Analytical solutions* Φ *of advection-diffusion problems in 1D depending on the mesh Reynolds number Re, and the left and right nodal values* Φ_l *and* Φ_r

Indeed, in the classical FV method the gradient term at each connecting link is modified by an upwind parameter α, which is given by the analytical solution of 1-D advection-diffusion problem (see also figure 3) :

$$\alpha = \coth\left(\mathrm{Re} - \frac{1}{\mathrm{Re}} \right) \quad \text{with: } \mathrm{Re} = \frac{\vec{u}_{ij}\Delta_{ij}}{\upsilon_{ij}} \qquad [11]$$

where Re is the non-dimensional Reynolds number and $\vec{\Delta}_{ij} = \vec{x}_i - \vec{x}_j$ is the coordinates vector from node j to node i. This scheme can be implemented straightforward with velocity $\vec{u}_{ij}$ and viscosity υ_{ij} evaluated amidst the links i-j as described above by using equation [6a] and the following expression:

$$(1-\alpha)\int_V \nabla\Phi_j \Phi_i dV \qquad [12]$$

Introducing this upwind scheme in the discretized linearized momentum equation [8] leads to following system:

$$\begin{aligned}
&\rho(\delta\vec{u})_i \int_V \Phi_i dV + \sum_{j\neq i}(1-\alpha)(\rho\vec{v})_{ij}\left[\left(\vec{u}_j^{\,n} - \vec{u}_i^{\,n}\right) + \theta\left(\delta\vec{u}_j - \delta\vec{u}_i\right)\right]\int_V \Phi_i \nabla\Phi_j dV \\
&+ \sum_{j\neq i}(\rho\upsilon)_{ij}\left[\left(\vec{u}_j^{\,n} - \vec{u}_i^{\,n}\right) + \theta\left(\delta\vec{u}_j - \delta\vec{u}_i\right)\right]\int_V \nabla\Phi_i \nabla\Phi_j dV \\
&+ \sum_{j\neq i}(\rho\vec{v})_{ij}\left[\left(p_j^n - p_i^n\right) + \theta\left(\delta p_j - \delta p_i\right)\right] = \rho_i \vec{g}\int_V \Phi_i dV, \text{ and} \\
&\sum_{j\neq i}\rho_{ij}\left[\left(\vec{u}_j^{\,n} - \vec{u}_i^{\,n}\right) + \theta\left(\delta\vec{u}_j - \delta\vec{u}_i\right)\right]\int_V \Phi_i \nabla\Phi_j dV = 0
\end{aligned} \qquad [12a]$$

3.2. *Stabilization by enrichment - the MINI element*

Furthermore, stabilized FE methods were investigated to overcome the deficiencies of the classical Galerkin method. They are consistent approaches leading to residual or sub-scale methods (Brezzi, Franca, Hughes, Russo 1996). In this framework bubble functions were introduced to circumvent the inf-sup condition in flow problems. Originally bubble functions were introduced to the FE method by Arnold and Brezzi (Arnold, Brezzi, Fortin, 1984) for Stokes flow. They enhanced the first order approximation of velocity by a function, which is 1 at the center of gravity of the element and 0 at its boundary. This MINI element is completed using first order approximation of pressure. This way an efficient coupling of velocity and pressure in the equation of continuity is obtained. Due to the enrichment of the velocity approximating space by bubble functions, this discretization fulfills the inf-

sup condition of Babuska – Brezzi (Gresho, Sani, 1998) resulting so in a stable finite element. Figure 2 shows schematically the unknowns and shape functions in 1-D.

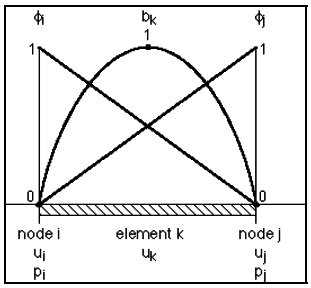

Figure 4. *MINI element in 1D using first order velocity plus bubble function and first order pressure approximations*

Due to the local effect of the bubble functions, which are defined only in the interior of each element, the bubble mode can be solved in dependency of the first order nodal values of the corresponding element. This way by so-called *static condensation* the degrees of freedom can be reduced to the same number as for first order discretizations. This way bubble stencils can be calculated according to the principles of the hybrid FE/FE method, thus leading to consistent stabilization terms.

After resolution the bubble modes usually are reconstructed. Numerical results show, that this reconstruction of the bubble function part of the solution even may be neglected (Soulaimani, Fortin, Quellet, Dhatt, Bertrand, 1987).

It has been shown, that this bubble stabilization reproduces the SUPG method. However, such classical bubble functions, which are used in the MINI element, only reproduce SUPG up to a certain Peclet or Reynolds number (Brezzi, Bristeau, Franca, Mallet, Rogé, 1992). With increasing advection the performance of classical bubbles deteriorates and the upwind stabilization feature is lost, even if the pressure stabilization still is obtained but pressure oscillations may occur at the boundaries. Therefore, modified or adapted bubbles, e.g. residual free bubbles (Hughes, 1995, Brezzi, Franca, Hughes, Russo, 1997, Franca, Nesliturk, Stynes, 1998), have been investigated by many researchers. But the development of adaptive residual free bubbles needs a severe extra effort in research, implementation and computational resources. A new way to obtain the stabilization of the MINI element over the whole range of Reynolds numbers will be presented in this work. Indeed, for increasing advection the stabilization by bubble functions will be limited by a classical pressure stabilizing Petrov-Galerkin (PSPG) scheme, initially introduced by Tezduyar *et al*. (Tezduyar, Mittal, Ray, Shih, 1992) (see paragraph 3.3).

3.3. *MINI volume elements in the hybrid FE/CV framework*

The concept of the MINI element has been implemented in the framework of the hybrid FE/FV method for the volume tetrahedron, pentahedron (prism) and hexahedron elements (Figure 5a-c). The transient linearized incompressible Navier-Stokes equation [1a] is the starting point to apply the concepts of the MINI element.

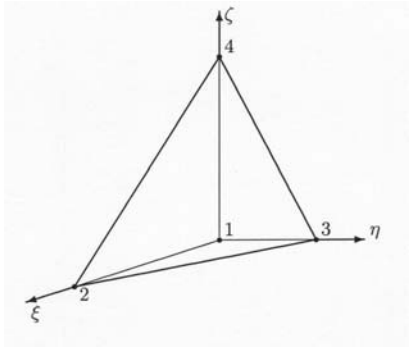

$$\Phi_1(\xi,\eta,\zeta) = 1-\xi-\eta-\zeta$$
$$\Phi_2(\xi,\eta,\zeta) = \xi$$
$$\Phi_3(\xi,\eta,\zeta) = \eta$$
$$\Phi_4(\xi,\eta,\zeta) = \zeta$$
$$b(\xi,\eta,\zeta) = 256\xi\eta\zeta(1-\xi-\eta-\zeta)$$

Figure 5a. *Tetrahedron element and the 4 linear shape functions* Φ_i *plus bubble function* b

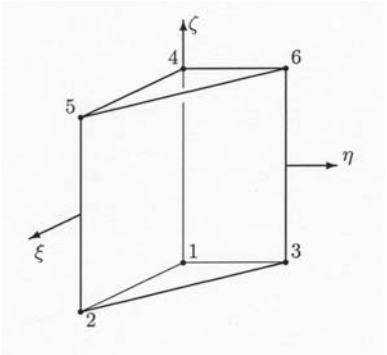

$$\Phi_1(\xi,\eta,\zeta) = \tfrac{1}{2}(1-\xi-\eta)(1-\zeta)$$
$$\Phi_2(\xi,\eta,\zeta) = \tfrac{1}{2}\xi(1-\zeta)$$
$$\Phi_3(\xi,\eta,\zeta) = \tfrac{1}{2}\eta(1-\zeta)$$
$$\Phi_4(\xi,\eta,\zeta) = \tfrac{1}{2}(1-\xi-\eta)(1+\zeta)$$
$$\Phi_5(\xi,\eta,\zeta) = \tfrac{1}{2}\xi(1+\zeta)$$
$$\Phi_6(\xi,\eta,\zeta) = \tfrac{1}{2}\eta(1+\zeta)$$
$$b(\xi,\eta,\zeta) = 27\xi\eta(1-\xi-\eta)(1-\zeta^2)$$

Figure 5b. *Pentahedron (prism) element and the 6 first order shape functions* Φ_i *plus bubble function* b

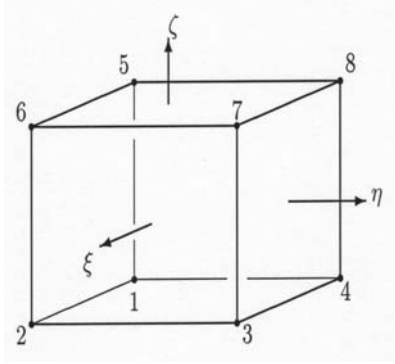

$$\Phi_1(\xi,\eta,\zeta) = \tfrac{1}{8}(1-\xi)(1-\eta)(1-\zeta)$$
$$\Phi_2(\xi,\eta,\zeta) = \tfrac{1}{8}(1+\xi)(1-\eta)(1-\zeta)$$
$$\Phi_3(\xi,\eta,\zeta) = \tfrac{1}{8}(1+\xi)(1+\eta)(1-\zeta)$$
$$\Phi_4(\xi,\eta,\zeta) = \tfrac{1}{8}(1-\xi)(1+\eta)(1-\zeta)$$
$$\Phi_5(\xi,\eta,\zeta) = \tfrac{1}{8}(1-\xi)(1-\eta)(1+\zeta)$$
$$\Phi_6(\xi,\eta,\zeta) = \tfrac{1}{8}(1+\xi)(1-\eta)(1+\zeta)$$
$$\Phi_7(\xi,\eta,\zeta) = \tfrac{1}{8}(1+\xi)(1+\eta)(1+\zeta)$$
$$\Phi_8(\xi,\eta,\zeta) = \tfrac{1}{8}(1-\xi)(1+\eta)(1+\zeta)$$
$$b(\xi,\eta,\zeta) = (1-\xi^2)(1-\eta^2)(1-\zeta^2)$$

Figure 5c. *Hexahedron element and the 8 first order shape functions* Φ_i *and bubble function* b

Again, an approximate static condensation is performed calculating a mean bubble degree of freedom. This is substituted into the continuity equation then to obtain a pressure stabilization.

The condensation is derived for each component of the advection-diffusion equations. To solve for the bubble mode $\vec{u}_k$ on element k, the Galerkin weak expression for the shape function b_k is considered for each component $I = x, y, z$ of the velocity field:

$$\begin{aligned}
&\sum_j \int \rho(\vec{u}_t^{\,I})_j\, dt \int_{V_k} b_k \Phi_j\, dV + \int \rho(\vec{u}_t^{\,I})_k\, dt \int_{V_k} b_k b_k\, dV + \\
&\sum_j \int \rho \upsilon \vec{u}_j^{\,I}\, dt \int_{V_k} \nabla\Phi_j \nabla b_k\, dV + \int \rho \upsilon \vec{u}_k^{\,I}\, dt \int_{V_k} \nabla b_k \nabla b_k\, dV + \\
&\sum_j \int \rho \vec{v} \vec{u}_j^{\,I}\, dt \int_{V_k} \nabla\Phi_j b_k\, dV + \int \rho \vec{v} \vec{u}_k^{\,I}\, dt \int_{V_k} \nabla b_k b_k\, dV + \\
&\sum_j \int p_j\, dt \int_{V_k} (\nabla\Phi_j b_k)^I\, dV = \sum_j \int \rho \vec{g}^{\,I}\, dt \int_{V_k} b_k \Phi_j\, dV \text{ with } I = x, y, z
\end{aligned} \qquad [13]$$

According to the principles of the developed FE/FV method, the thermo-physical properties can be approximated by homogenized values. Static condensation is then applied to the bubble terms of equation [13]. This solution is performed only approximately resulting in a mean bubble mode integrated over each time step. As no determination of the bubble mode values is required, the change of the bubble mode values during a time-step is neglected:

$$\int \rho(\vec{u}_t^{\,I})_k \, dt \int_{V_k} b_k b_k \, dV \approx 0 \qquad [14]$$

This way the static condensation is reduced to a simpler task. Equation [13] is then solved for the mean bubble term leading to:

$$\left(\vec{U}_k\right)^I := \int \vec{u}_k^{\,I} dt \approx \frac{1}{\int_{V_k} \nabla b_k \nabla b_k \, dV} \begin{pmatrix} + \sum_j \int \frac{1}{\upsilon} \vec{g}^{\,I} dt \int_{V_k} b_k \Phi_j \, dV \\ - \sum_j \int \frac{1}{\upsilon} (\vec{u}_t^{\,I})_j \, dt \int_{V_k} b_k \Phi_j \, dV \\ - \sum_j \int \frac{\vec{v}}{\upsilon} \vec{u}_j^{\,I} dt \int_{V_k} \nabla \Phi_j b_k \, dV - \\ \sum_j \int \frac{1}{\rho \upsilon} p_j dt \int_{V_k} \left(\nabla \Phi_j b_k\right)^{\mathrm{T}} dV \end{pmatrix} \qquad [15]$$

Using this result the discretized incompressible Navier-Stokes equation can be stabilized. Stabilization is there required for two kinds:

– momentum equation due to advection-diffusion;

– continuity equation needs a pressure stabilization.

The upwind stabilization for the momentum equation is obtained using a conventional upwind scheme, which is regarded to be advantageous compared to classical bubble functions. Therefore bubbles are selected for pressure stabilization purposes only. Hence for stabilizing the continuity equation, an adaptive approach was selected. According to the local Reynolds number either the stabilization is performed by the bubble functions or by the PSPG method. Thus a stable discretization is realized for the whole range of possible Reynolds numbers.

3.4. *Pressure stabilization of the continuity equation*

The condensed mean bubble mode is substituted into the continuity equation $\nabla \cdot \vec{u} = 0$. This leads to an enhanced equation:

$$\sum_I \left(\sum_j \sum_k \int \vec{u}_j^I dt \int_{V_k} \nabla \Phi_j \Phi_i \, dV + \sum_k \vec{U}_k^I \int_{V_k} \nabla b_k \Phi_i \, dV \right) = 0 \qquad [16]$$

By introducing the mean bubble mode $\vec{U}_k^I$ [15] the stabilizing enhancement term [17] is derived. Additionally $\int_{V_k} \nabla b_k \Phi_i dV = -\int_{V_k} b_k \nabla \Phi_i dV$ is there applied, leading to:

$$
\begin{aligned}
&+\sum_I \sum_j \int \tfrac{1}{\upsilon} (\vec{u}_t)_j^I dt \sum_k \frac{\int_{V_k} \Phi_j b_k dV}{\int_{V_k} \nabla b_k \nabla b_k dV} \int_{V_k} \left(b_k \nabla \Phi_i\right)^I dV \\
&+\sum_I \sum_j \int \tfrac{\dot{\nu}}{\upsilon} \vec{u}_j^I dt \sum_k \frac{\int_{V_k} \nabla \Phi_j b_k dV}{\int_{V_k} \nabla b_k \nabla b_k dV} \int_{V_k} \left(b_k \nabla \Phi_i\right)^I dV \\
&+\sum_I \sum_j \int \tfrac{1}{\rho\upsilon} p_j dt \sum_k \frac{\int_{V_k} \left(\nabla \Phi_j b_k\right)^I dV}{\int_{V_k} \nabla b_k \nabla b_k dV} \int_{V_k} \left(b_k \nabla \Phi_i\right)^I dV \\
&-\sum_I \sum_j \int \tfrac{1}{\upsilon} \vec{g}^I dt \sum_k \frac{\int_{V_k} \Phi_j b_k dV}{\int_{V_k} \nabla b_k \nabla b_k dV} \int_{V_k} \left(b_k \nabla \Phi_i\right)^I dV
\end{aligned}
\qquad [17]
$$

Since the bubble function stabilization is limited to a certain degree of advection, a limiting switch will be introduced. The terms resulting from bubble function stabilization occur in similar form, if a Pressure-Stabilizing-Petrov-Galerkin (PSPG) method (Tezduyar, Mittal, Ray, Shih, 1992) is applied. This stabilization method uses also first order shape functions and is constructed analogously to SUPG or other stabilizing methods for FE. PSPG consists of the addition of a parameterized divergence of the momentum residual to the continuity equation:

$$\nabla \cdot \vec{u} - \tfrac{\tau}{\rho} \nabla \cdot (\text{momentum residual}) = 0 \qquad [18]$$

with τ a stabilizing parameter

The choice of this parameter will be discussed later. At first, the discretization of the stabilization equation [18] will be considered. The residual $R(\vec{u}, p)$ of the linearized momentum equation is formed as following:

$$R(\vec{u}, p) = \rho \vec{u}_t + \rho(\vec{v} \cdot \nabla)\vec{u} - \rho\upsilon\Delta\vec{u} + \nabla p - \rho\vec{g} \qquad [19]$$

Then the stabilization $S(\vec{u}, p)$ is given by [20], which is used as starting point for the subsequent FE discretization:

$$S(\vec{u}, p) = -\tau\nabla \cdot \vec{u}_t - \tau\nabla \cdot (\vec{v} \cdot \nabla)\vec{u} - \tau\nabla \cdot \upsilon\Delta\vec{u} - \tfrac{\tau}{\rho}\nabla \cdot \nabla p + \tau\nabla \cdot \vec{g} \qquad [20]$$

Using first order shape functions, the term $\nabla \cdot (\upsilon\Delta\vec{u})$ cannot be discretized. Thus it has been neglected in this method, which relies on first order functions only. Then

4 terms are introduced into the enhanced continuity equation. These terms are discretized applying the hybrid FE/FV methodology described in paragraph 2. Thus the usual stencils can be reused and matrix assembly is simplified to the combination of stencils, thermo-physical data and of the stabilizing parameter τ . As for other stabilization methods of Petrov-Galerkin type, PSPG depends on the stabilization parameter τ . The proper choice of τ is crucial for the performance of this method. Again several selections of τ are proposed in the literature. Tezduyar *et al*. 1992 suggest to adopt the same choice as for SUPG in the momentum equation.

Using these definitions forms, which are more suitable for their implementation, one can deduce:

$$\tau_{PSPG} = \sqrt{\frac{4}{(\Delta t)^2} + \frac{4|\vec{u}|^2}{h^2} + \frac{36\upsilon^2}{\rho^2 h^4}}^{-1} = \frac{\Delta t}{2}\sqrt{1 + C^2 + 6\left(\frac{\upsilon}{\rho h^2}\right)^2}^{-1} \qquad [21]$$

where C is the element Courant number and h is the inner diameter of the element.

It follows from [21], that the stabilization parameter τ is always less than Δt . In the limit of a vanishing time-step, the introduced stabilization reduces to zero. Thus the PSPG stabilization constitutes a consistent perturbation.

The calculation of τ is different in the FE/FV framework as in a pure FE approach. Within the FE method the stabilizing parameter τ is calculated for each element and h is there the inner elemental diameter. However within the FE/FV framework, the stabilization is associated to the links between neighboring nodes. The element diameter h is interpreted here as the nodal distance. Thus h becomes the distance between nodes i and j: $h := \left|\vec{\Delta}_{ij}\right| = \left|\vec{x}_i - \vec{x}_j\right|$. The thermo-physical properties ρ, υ and the linearized velocity $\vec{v}$ are evaluated as averaged values amidst the link i-j. This way the stabilization parameter τ_{ij} is evaluated as following:

$$\tau_{ij} = \frac{\Delta t}{2}\sqrt{1 + C_{ij}^{\ 2} + 6\left(\frac{\upsilon_{ij}}{\rho_{ij}\left|\Delta_{ij}\right|^2}\right)^2}^{-1} \qquad [22]$$

The diagonal stabilizing parameter is defined according to the FE/FV principles analogously to [4] using expression [22]:

$$\tau_{ii}\int_V \Phi_i \nabla\Phi_i dV = -\sum_{j\neq i}\tau_{ij}\int_V \Phi_i \nabla\Phi_j dV \qquad [23]$$

This way the PSPG stabilization term is now discretized completely. Applying both the common Galerkin weak form and the partial integration, the hybrid FE/FV formulation of the PSPG method becomes:

$$
\begin{aligned}
&-\sum_I \sum_j \tau_{ij} \int_{t_n}^{t_{n+1}} \left(\vec{u}_j\right)_t^I \sum_k \int_{V_k} \left(\nabla \Phi_j\right)^I \Phi_i dV dt \\
&+\sum_I \sum_j \tau_{ij} \int_{t_n}^{t_{n+1}} \left(\vec{u}_j\right)^I \vec{v}_{ij} \sum_k \int_{V_k} \nabla \Phi_j \left(\nabla \Phi_i\right)^I dV dt \\
&+\sum_j \tau_{ij} \int_{t_n}^{t_{n+1}} p_j \sum_k \int_{V_k} \nabla \Phi_j \nabla \Phi_i dV dt \\
&+\sum_I \sum_j \tau_{ij} \int_{t_n}^{t_{n+1}} \left(\vec{g}\right)^I \sum_k \int_{V_k} \left(\nabla \Phi_j\right)^I \Phi_i dV dt
\end{aligned}
\qquad [24]
$$

The form of the stabilization terms again reveals the similarity of PSPG and bubble functions. In this new approach the continuity equation is stabilized either by bubble functions or by PSPG. Indeed, a switch from condensed bubble functions to the PSPG stabilization is introduced to ensure a stabilized FE/FV method for the whole range of possible Reynolds numbers. When the Reynolds number increases, the bubble function stabilization is selected only if their absolute values are less than the absolute values of the related PSPG terms. As for large Reynolds numbers the value of the bubble term becomes also large, the PSPG terms are then used to stabilize the continuity equation.

The introduction of this adaptive stabilization scheme enhances the equal order discretization. In a separate procedure the stabilization is added to the global system. For each link from node i to node j the local bubble and PSPG stabilization terms are calculated including the calculation of the local stabilization parameter τ_{ij}. After calculating the bubble function terms and the PSPG stabilization, the switch is applied to select the kind of stabilization, which is introduced into the system.

4. Application of the stabilized method to fluid flow problems

To evaluate the feasibility of the developed hybrid FE/FV method two typical configurations occurring in fluid flow were investigated: isothermal flow over a backward facing step and thermal convection in a cube. Each of the selected configurations represents a special part of industrial processes. If they are solved accurately, a proper solution of complex processes may be possible. Since a tetrahedral enmeshment needs special stabilization both tests were performed using tetrahedral meshes to demonstrate the capabilities of the developed stabilized FE/FV

method. Within this paper the results on the isothermal flow over a backward facing step are presented here. For details see (Neises, Stemmler, Laschet, 1999, Neises, 2001).

Flow over a backward facing step is a common test case, which was studied thoroughly by experiments and simulation. Therefore it was selected as first test case. To analyze the features of the new stabilized method, isothermal flow is only considered. This way the influence of heat transfer is neglected and fluid flow is tested in an isolated manner.

The domain of flow is basically rectangular. A channel is configured to model the flow into the domain. After some distance the inflow channel widens in one direction, this way it forms a step illustrated in figure 6. At the inflow surface a parabolic velocity profile is assumed, which is characteristic for flow in such a channel.

Behind the step the characteristic flow pattern depends on the Reynolds number. For very low Reynolds numbers, the flow attaches smoothly to the wider domain. No recirculation is there observed in experiments. For higher Reynolds numbers a recirculation zone with a vortex forms. The vortex enlarges with increasing advection and velocity.

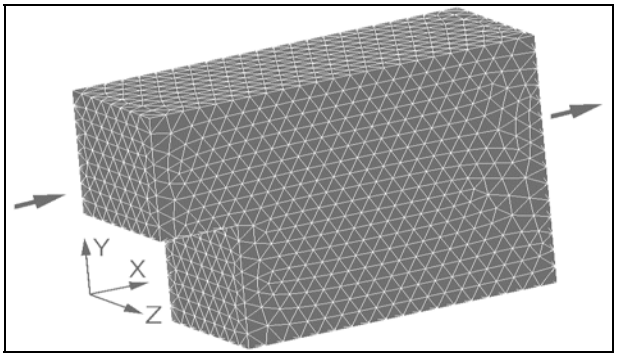

Figure 6. *Enmeshment of the backward facing step. The mesh consists of 3030 nodes and 13685 tetrahedrons*

Material data, similar to common metallic melts, were used in this simulation: density $\rho = 4$ g/cm^3 and the kinematic viscosity $\nu = 0.01$ cm/sec. The model got the following dimensions:

– length of the complete model (x)	15 cm
– step depth	3 cm
– step ratio (h/d)	5/3
– heigt (y)	10 cm
– width (z)	5 cm

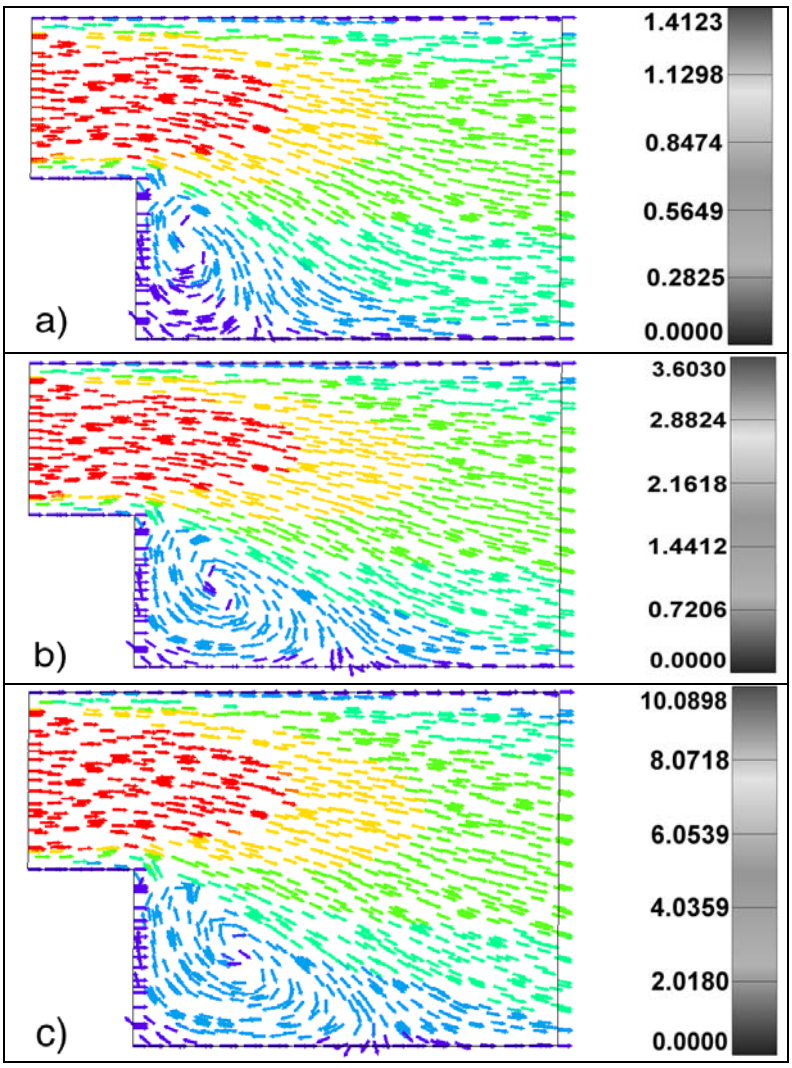

Figure 7. *The steady state flow field at a cross-section parallel to the x-y plane in the middle of the geometry is presented for different velocities at the inlet. The backward facing step is calculated using inlet velocities of (a) 1 cm/s, (b) 2 cm/s and (c) 4 cm/s*

This step domain has been enmeshed with tetrahedrons leading to a model of 3030 nodes and 13685 elements (Figure 6). Due to actual preprocessing possibilities only a uniform velocity has been set at the inlet boundary. An outflow boundary condition, modeling free flow and imposing just the pressure boundary condition of

equation [10], has been imposed at the outlet. At the other walls no-slip conditions have been defined. Velocities of 1 cm/s (Figure 7.a), 2 cm/s (Figure 7.b), 4 cm/s (Figure 7.c) leading to Reynolds numbers of 140, 280 and 560 have been tested. The numerical results show the experimentally known characteristics. In figure 7 the velocity is presented by arrows of equal length indicating the speed by color varying from blue (zero velocity) to red (high velocity).

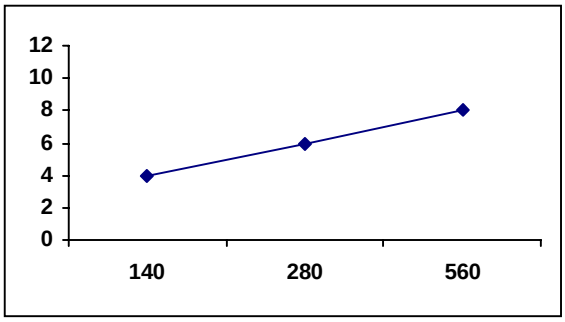

Figure 8. *Reattachment length in cm depending on the Reynolds number*

The imposed uniform velocity at the inlet evolves to a parabolic profile above the step. At the outlet a parabolic profile is also observed according to the colors variation. As expected the peak velocity at the outlet lower is than at the inlet due to the widened channel. The Dirichlet boundary condition leads to artificial arrows. Below the step a recirculation zone with a vortex is obtained. A small vortex forms by a velocity of 1 cm/s at the inlet. With increasing velocity and Reynolds number the vortex enlarges. The reattachment length increases linearly in respect with the Reynolds number (see Figure 8). Thus the stabilized method reproduces qualitatively the characteristic flow pattern for this test.

5. Modeling of free surfaces

Due to the simultaneous coupled occurrence of physical phenomena, each of which is a challenge in numerical simulation, mold filling is a very difficult task in casting process simulation. Indeed, these phenomena range from transient multiphase incompressible flow, interface kinetics and dynamics, heat transfer, which consists of convection-diffusion and radiation problems, to phase change including multiple components and microstructural phenomena, and finally thermo-mechanical effects. Much work is needed before this nonlinearly coupled problem can be analyzed completely. However, numerical simulation of mold filling provides a tool to gradually gaining further insight into the mechanisms taking place and understanding these complicated interfacial flows (Kothe, Juric, Lam, Lally, 1998).

5.1. *The VoF method*

Among the methods used to model interfacial flows, interface capturing methods are rather popular and wide spread especially within the finite volume community. Since the first publication of volume tracking methods, *i.e*. the volume of fluid (VoF) method, over two decades ago it has proven to be a useful and robust tool, which has been improved by several enhancements (Kothe, Rider, 1995). Thus it becomes a frequent choice in Eulerian models of interfacial flows, especially where interfaces undergo topology changes. In the VoF interface tracking method the initial interface geometry is used to compute fluid volume fractions F in each computational cell or finite volume. This task amounts to computing the volume truncated by the fluid interface in each cell containing an interface. Exact interface information is discarded in favor of the discrete volume fraction data. Interfaces are subsequently tracked by evolving fluid volumes in time with the solution of a standard convection equation (Kothe, Rider, 1995):

$$\frac{\partial F}{\partial t} + \vec{u} \cdot \nabla F = q \text{ , with } q \text{ a source term} \qquad [25]$$

Volume fractions result from normalization of fluid volumes relative to the cell control volume, *i.e.* $F = 1$ means full and $F = 0$ means empty. An exact interface location is not known. A location of the interface is reconstructed from local volume fraction data. Without reconstruction even high order advection schemes show an excessive amount of numerical diffusion, if they are applied to mold filling. However, any reconstruction based concept is related to geometrical concepts. Thus such an approach does do not fit into the hybrid FE/FV framework of CASTS using virtual finite volumes without any geometrical description. Therefore a new stabilization scheme, which can be used on unstructured meshes without any reconstruction on cell level, was developed (Neises, Laschet, 1998a). This stabilization scheme, named “FF-VoF method”, is implemented in CASTS.

5.2. *The FF-VoF method*

The FF-VoF stabilization scheme is based on the thermodynamic concept of minimal free energy at the surface. The main principles were developed in the phase field theory (Steinbach, 2000). The phase field approach was applied to the VoF method as a consistent perturbation of the transport equation. The main features of the phase field concept are:

– the sharp interface is modeled as a smooth transition over a thin layer;

– the interfacial dynamics are treated by interfacial forces, *i.e*. diffusive and anti-diffusive forces, which cancel each other at equilibrium.

The FF-VoF method uses the Gibbs-Thompson relations and the description of the interface free energy as a model for the liquid-gas interface. The phase field is interpreted as a fluid field. The microscopic phases liquid and solid are referred to the macroscopic liquid and gas phases. If the interface is planar, the diffusive and the source term cancel each other in equilibrium. Therefore the interfacial energy may be considered as a consistent perturbation. Thus a surface potential consisting of diffusion and molecular forces was added to the transport equation [25] of the filling function F stabilizing the numerical solution of the purely advective transport equation transforming it into an advection-diffusion equation. Using this approach the reconstruction on cell level was avoided. For details, please, refer to (Neises, Laschet, 1998), (Laschet, Neises, Diemer, 1998b) or (Neises, 2001). The modified transport equation of FF-VoF is given by:

$$\frac{\partial F}{\partial t} + \vec{u}\nabla F = q + \varepsilon\nabla^2 F - \beta F(1-F)(\frac{1}{2} - F) \qquad [26]$$

A similar enhancement of the transport equation is derived by the model of continuous surface force (CSF) developed by Kothe *et al*. (Kothe, Juric, Lam, Lally 1998).

By varying locally the parameters ε and β, the interface region can be adopted to the mesh. The width of the interface is controlled by diffusion and molecular forces. The transition - $0.05 < F < 0.95$ - has a characteristic thickness of

$$\delta = 6\varepsilon\sqrt{2\beta^{-1}} \qquad [27]$$

The parameters are controlled locally by the size of the elements. In a first approach global values are calculated by adopting $\varepsilon = \beta$. The parameters are calculated using an estimation of the desired interfacial width. The interface should be spread over 3 to maximum 5 cells. Thus the width δ should not be larger than 3 times the minimal cell width, but it may be about 2 times the average cell width. The cell width is defined accordingly to the FE/FV approach as the distance between adjacent nodes Δ_{ij}. As equal diffusive and molecular forces are assumed, equation [27] reduces to:

$$\min\left(3 \cdot \min\left(\Delta_{ij}\right), 2 \cdot \mathrm{ave}\left(\Delta_{ij}\right)\right) = \delta = 6\varepsilon\sqrt{2\varepsilon^{-1}} \text{ and } \varepsilon = \beta \qquad [28]$$

This way, a fixed transition zone of a few elements thickness for unstructured meshes is obtained efficiently. Additionally, the computational domain is defined by cells, which are filled more than an adjustable minimal degree of at least 5%. The free surface is defined by the nodes, which at least have one neighbor, which is outside the computational domain.

Since the modified differential equation is rather *parabolic* than hyperbolic, some numerical difficulties, such as sophisticated advection schemes, drop. Furthermore, existing routines modeling the parabolic heat transfer problem can be easily reused. Consequently the changes of the code to implement FF-VoF in CASTS are limited to few routines. The implementation of the FF-VoF method follows the principles of the hybrid FE/FV method. A segregated approach is selected to calculate the solution of the coupled problem. The stabilized FF-VoF equation [26] is discretized analogously to the likewise parabolic equation of heat transfer. Only the treatment of the changing calculation domain needs special attention.

6. The MCWASP mold filling benchmark

At the 7th conference on Modeling of Casting, Welding and Advanced Solidification Processes (Sirrel, Holliday, Campbell, 1995) results of a benchmark problem of mold filling were presented. Numerical modeling was tested against a well defined experiment, which was documented by x-ray radiography. This benchmark is well documented and allows a very good evaluation of any mold filling simulation program like CASTS rev. 12.4. For its design two requirements had to be fulfilled. The selected geometry of the casting should be simple to ensure reproducible experiments, but it needed to be sufficient complex to result in a fastidious numerical test. Therefore a tall sprue was selected (see Figure 9). From previous experiments it was known that such a sprue results in a high turbulence in the runner and the gate.

For this benchmark approximately 2.2 kg of aluminium were poured into a pouring basin on top of the sprue. When this basin was full, a stopper was lifted abruptly, thus starting the filling of the mold. The melt entered the sprue at about 700°C. The pouring continued uninterrupted for about 3.5s. The lifting of the stopper was set at time zero. Then each 0.02s an x-ray video frame was taken during the filling process. The experiment was repeated several times to ascertain its reproducibility. Three examples were selected and published (Sirrel, Holliday, Campbell, 1995). Comparison of this synopsis shows a qualitative agreement of the filling patterns in the selected experiments. Nevertheless the patterns differ when the melt fills the runner and enters the gate. This is mainly caused by the degree of turbulence occurring during this part of the filling. However, within all experiments a filling time of 2.24s was observed. For detailed data on the mold's size and the used thermo-physical data, please refer to (Sirrel, Holliday, Campbell, 1995) or (Neises, 2001).

The mold has been discretized by a mesh of 7740 hexahedrons and 10224 nodes (Figure 8). No slip boundary conditions are imposed. The pouring basin is kept full during filling. Vacuum is assumed within the mold. Additionally two simplifying assumptions are made. First, isothermal flow is assumed. Second, separation and solidification of mold material is not modeled. In table 1 the used boundary conditions, time step sizes and numerical parameters are summarized.

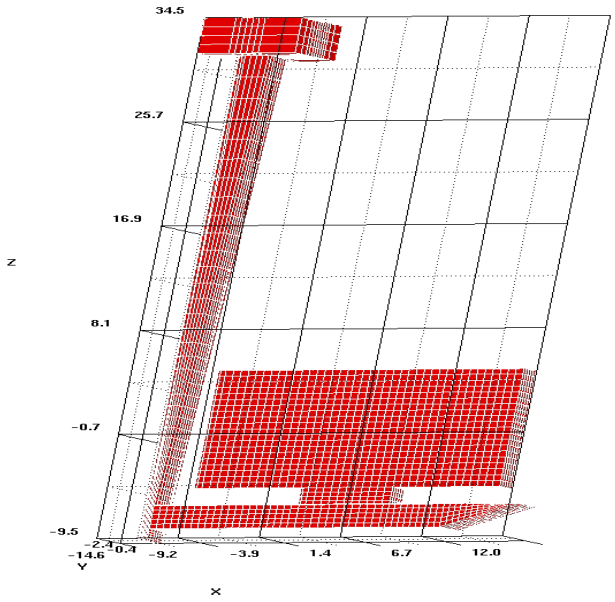

Figure 9. *The geometry and the FE-enmeshment of the mold filling benchmark*

The stabilized method shows a thinning profile when the melt falls down the sprue. The front remains compact. High velocities occur when the melt leaves the sprue and enters the runner after about 0.26s (Figure 10a), even if a longer time might be expected due to the no-slip boundary condition, which lets filling take part only at the inner virtual cells. This time almost agrees with experimentally measured 0.24s. Entering the runner, the melt fills the bottom of the runner first (Figure 10b). A vortex is observed at the top edge of the runner's entry. A second vortex forms at the bottom of the sprue. Due to the high velocities the front still is smeared over the whole cross-section of the runner (Figure 10c) instead of leaving the top part of the runner unfilled. However, due to the vorticity at the edge connecting sprue and runner, an empty region is observed.

Then the melt fills the complete runner from the entry to the end. The end is reached at about 0.45s (Figure 11a) in agreement with the experiment. Since the front is smeared, the melt starts piling up into the gate before the end of the runner is reached. Entering the plate, the melt forms the characteristic mushroom front type (Figure 11b). Then it spreads aside and swashes against the left and right wall rising there (Figure 10c). This is also observed experimentally.

Finally an almost planar front is formed (12a) and the plate is filled vertically. The whole plate is filled after 2.65s (12b). Thus using the stabilized equal order method the patterns agree with the experiments.

Table 1. *Computational parameters used within the simulation of the MCWASP benchmark*

Number of nodes and elements	10224 nodes and 7740 hexahedrons
Boundary conditions	No-slip at the walls Free flow at inlet and the free surface Zero pressure at the free surface
Initial condition	The bassin is filled.
FF-VoF parameter	$\varepsilon = \beta = \frac{1}{800}$
Time steps	0.005s from 0.00s up to 0.14s 0.002s from 0.14s 0.25s 0.001s from 0.25s to 3.00s

To demonstrate the capabilities of the proposed stabilized FE/FV method the obtained filling time is compared to published results (see table 2) (Cross, Campbell 1995). Still the achieved filling time of 2.65s deviates by 18.3% from the experimentally obtained filling time of 2.24s and compared with 2.2s obtained using LS-DYNA3D. But this result was obtained without any optimization of numerical parameters. This way the time consuming search of a suitable set of parameters drops. Automatic time stepping will improve the simulation, since the simulation was performed using only one iteration per time step. However, the result suffers from several simplifications:

– The basin is modeled in a very simplified manner and the 2nd fluid (air) is not modeled;

– The outflow boundary condition at the free surface requires to be improved;

– The no-slip boundary condition at the walls is not suitable for coarse meshes and a slip boundary condition is required instead.

Hence improved boundary conditions are very important tasks in further development.

Table 2. *Filling times for the benchmark problem calculated by several simulation tools*

PROGRAM	Filling Time	Deviation from Experiment
Flow-3D	1.83s	22.4%
WTCM perfect slip condition	2.15s	4.1%
LS-DYNA3D	2.2s	1.8%
Experimental results	2.24s	0%
WTCM no slip condition	2.33s	6.25%
CASTS stabilized FE/FV	2.65s	18.3%
FIDAP	4.0s	78.5%

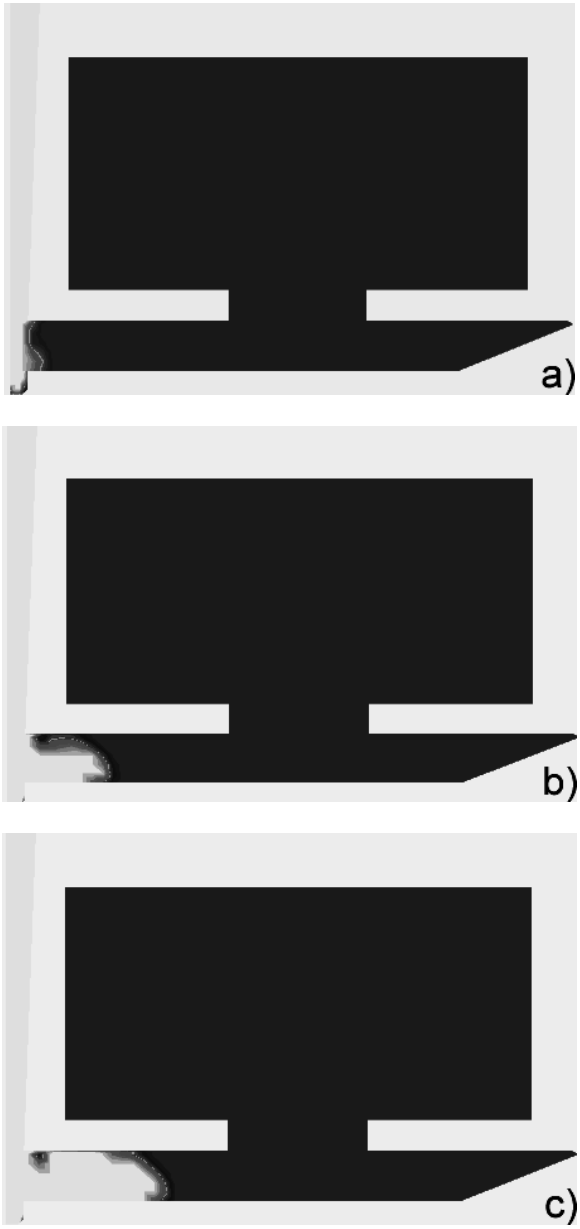

Figure 10. *Numerical results achieved using the stabilized FE/FV method. The melt leaves the sprue (a) and enters the runner (b). Still the transition region remains compact (c)*

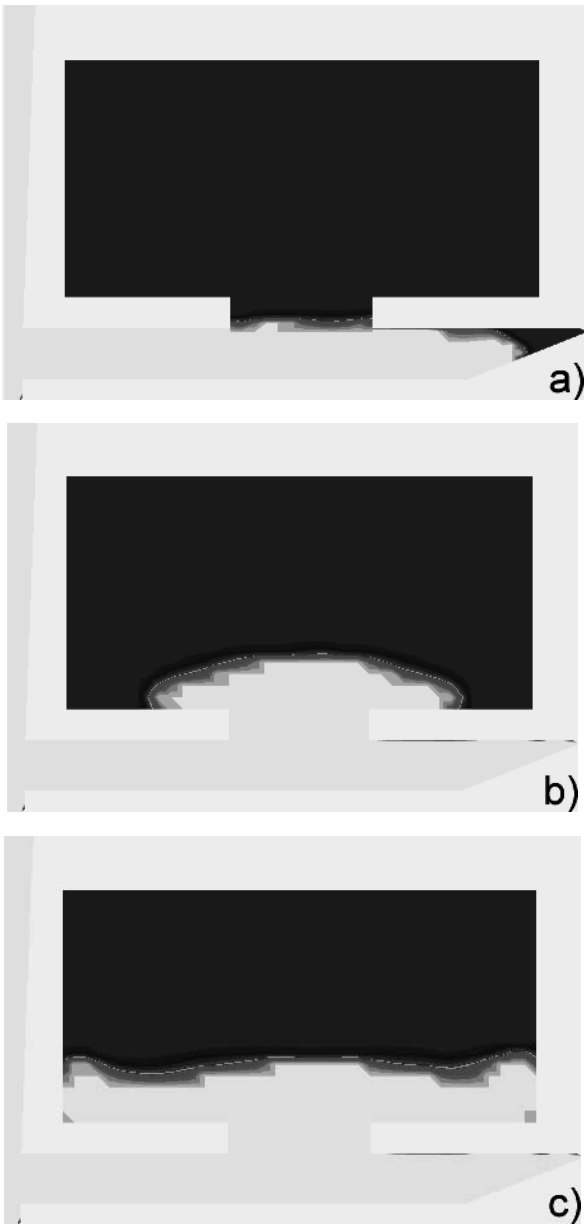

Figure 11. *Numerical results achieved using the stabilized FE/FV method. The plate is entered by the melt (a). The melt flows aside and the front flattens (b). When the melt reaches the sides of the plate it rises and splashes back (c)*

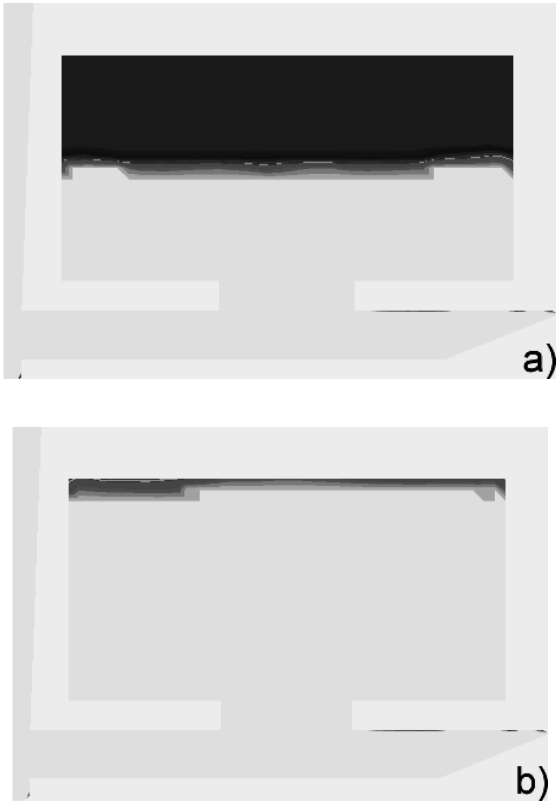

Figure 12. *The plate is filled vertically (a). An almost plane front is observed. Using the stabilized FE/FV method the plate is filled at 2.65 seconds (b)*

Since the benchmark is a challenging problem and several simplifying assumptions have been made (e.g. laminar flow, no-slip boundary condition), it will be a remaining test for ongoing developments. The FF-VoF volume tracking method still leads to a smearing of the front in the runner. The filling pattern is not well reproduced there. Furthermore, the boundary conditions at the free surface still are open issues. Finally, due to the no-slip boundary condition the boundary layer cannot be resolved, if coarse meshes are used. The fractional step approach coupling the flow field and mass transport still leads to small times steps due to the hyperbolic kind of the transport equation and the predicted filling times depend strongly on the selected time stepping. Therefore improvements of the solution of mass transport and the treatment of free surfaces in general need further investigations.

7. Conclusions

A new flow solver applicable to casting processes has been presented here. This solver is achieved by introducing an equal order approximation and stabilized FE methods into the hybrid FE/FV framework established within the simulation tool CASTS rev 12.4. Using bubble functions and static condensation a consistent pressure stabilization is achieved. To ensure the stabilizing properties for high Reynolds numbers, the bubble function terms are limited locally by a pressure stabilizing Petrov-Galerkin method. Then, a new stabilization of the filling front is presented based on phase field concepts.

The MCWASP benchmark problem has been performed. The simulated flow and filling patterns agree with experimental results. Only the highly turbulent regime, when the melt enters the runner, leads to a smearing of the interface by the implemented FF-VoF method. Nevertheless, due to the boundary conditions at the free surface and the fractional step type coupling of the fluid flow and transport modules, a deviation of 18% from the experimental time is only observed. This predicted time is within the range obtained by other commercial simulation programs. The table of results illustrates, that consideration of sophisticated tasks as modeling turbulence, multiphase flow and the choice of boundary conditions significantly influence the result in filling time. Nevertheless, the implementation of the new stabilization scheme in the hybrid FE/FV framework of CASTS leads to a simulation tool suitable to model the mold filling of complex casting parts.

8. References

Arnold D. N., Brezzi F., Fortin, M., "A stable finite element for the Stokes equations", *Calcolo 23*, Vol. 4, 1984, pp. 337-334.

Brezzi F., Bristeau M.-O., Franca L. P., Mallet M., Rogé P., "A relationship between stabilized finite element methods and the Galerkin method with bubble functions", *Comput. Meth. Appl. Mech. Eng*., 1992, pp. 117-129.

Brezzi F., Franca L. P., Hughes T. J. R., Russo A., "Stabilization Techniques and Subgrid Scale Capturing", *Proceedings of the Conference on the State of the Art in Numerical Analysis, York, England*, IMA Conference Series, Vol. 63 (Duff, I.S. and Watson, G. A. eds.), Oxford University Press, April 1996, pp. 391-406.

Brezzi F., Franca L. P., Hughes T. J. R., Russo A., "$b = \int g$", *Comput. Meth. Appl. Mech. Eng.*, Vol. 145, 1997, pp. 329-339.

Brooks A. N., Hughes T. J. R., "SUPG formulations for convection dominated flows with particular emphasis on the incompressible Navier-Stokes equations", *Comput. Meth. Appl. Mech. & Eng.*, Vol. 32, 1982, 199-259.

Cross M., Campbell L., (eds.): *Proceedings of Modeling of casting, welding and advanced solidification*, TMS publications, 1995.

Dhatt G., Gao D. M., Ben Cheikh A., "A Finite Element Simulation of Metal Flow in Moulds", *Int. J. Num. Meth. Eng.*, 30, 1990, pp. 821-831.

Donea J., "A Taylor-Galerkin Method for Convective Tramsport Problems", *Int. J. Num. Meth. Eng.*, 20, 1984, pp. 101-119.

Franca L. P., Frey S. L., Hughes T. J. R., "Stabilized finite element methods: I. Application to the advective-diffusive model", *Comput. Meth. Appl. Mech. Eng.*, 95, 1992, pp. 253-276.

Franca L. P., Frey S. L., "Stabilized finite element methods: II. The incompressible Navier-Stokes equations", *Comput. Meth. Appl. Mech. Eng*., 99, 1992, pp. 209-233.

Franca L. P., Russo A., "Deriving Upwinding, Mass Lumping and Selective Reduced Integration by Residual Free Bubbles", *Appl. Math. Letters*, 1996.

Franca L. P., Nesliturk A., Stynes M., "On the stability of residual-free bubbles for convection-diffusion problems and their approximation by a two-level finite element method", *Comput. Meth. in Appl. Mech. Eng*., 1998, pp. 35-49.

Gresho P. M., Sani B., *Incompressible Flow and the Finite Element Method* – Haldenwanger A., Stich A., "Casting Simulation an an Innovation in the Motor Vehicle Development Process", *in: Proc. of MCWASP - IX*, Sahm, P. R., Hansen, P. N., Conley, J. G. (eds.), Shaker Verlag, pp. XLIV-LI, 2000.

Huerta A., Roig B., Donea J., "Time-Accurate Solution of Convective Transport Problems", ECOMAS 2000, http://www-lacan.upc.es/lacan/articulos/pdf/eccomas2000_huerta_hrd.pdf

Hughes T. J. R., "Multiscale phenomena: Green's functions, the Dirichlet-to-Neumann formulation, subgrid scale models, bubbles and the origin of stabilized methods", *Comput. Meth. Appl. Mech. Eng*., 127, 1995, pp. 387-401.

Idelsohn S. R., Oñate E., "Finite Volumes and Finite Elements 'Two good Friends'", *Int. J. Numer. Meth. Eng.*, 37, 1994, pp. 3324-3341.

Kothe D. B., Rider W. J., Comments on Modeling Interfacial Flows with Volume-of-Fluid Methods, http://public.lanl.gov/mww/HomePage.html.

Kothe D. B., Juric D., Lam K., Lally B., Numerical Recipes for Mold Filling Simulation, http://public.lanl.gov/mww/HomePage.html.

Laschet G., Neises J., Steinbach I., "Micro and Macrosimulation of Casting Processes", *in: 4^{e} école d´été du GUT, Modélisation numérique en thermique*, Lecture Notes, Porquerolles, 1998.

Laschet G., Neises J., Diemer M.: "Simulation of Casting Processes with CASTS", *in: 4^{e} école d´été du GUT, Modélisation numérique en thermique*, Workshop, Porquerolles, 1998.

Morton K. W., Parrott A. K., "Generalized Galerkin Methods for First Order Hyperbolic equations", *J. Comp. Phys.*, 36, 1980, pp. 246-270.

Neises J., Steinbach I., "Finite Element Integration for the Control Volume Method", *Comm. Num. Meth. Eng.*, 12, 1996, pp. 543-555.

Neises J., Laschet G., A Fluid Field Method for Transient Free Surfaces, ACCESS, Annual Report of DFG-CNRS project on numerical free surface flow, 1998.

Neises J., Steinbach I., Delannoy Y., "Modeling of Free Surfaces in Casting Processes", in*:* Notes on *Numerical Fluid Mechanics, Vieweg,* 1998, pp. 168-186.

Neises J., Stemmler M., Laschet G., "A hybrid Control-Volume Method stabilized by Bubble Functions applied to Fluid Flow" in *Casting Processes, USNCCM99,* Book of Abstracts, 1999, pp. 221.

Neises J., Numerical Modeling of Incompressible Flow Applied to Casting Processes, PhD thesis, Technical University of Aachen, 2001, http://www.bth.rwth-aachen.de/job/disslist.pl

Patankar S. V., *Numerical Heat Transfer and Fluid Flow*, Hemisphere, 1980, Washington D.C.

Sahm P. R., Hansen P. N., "Towards Integrated Modeling for Intelligent Castings", *in: Proc. of MCWASP - IX*, Shaker Verlag, pp. XLIV-LI, 2000, LXXXI.

Sirrel B., Holliday M., Campbell J., "The benchmark test 1995", *Proc. 7th Int. Conf. on Modeling of Casting, Welding and Advanced Solidification Processes*, TMS 1995, pp. 915-932.

Song R., Dhatt G., Ben Cheikh A., "Thermo-Mechanical Finite Element Model of Casting Systems", *Int. J. Num. Meth. in Eng.*, Vol. 30, 1990, pp. 559-579.

Soulaimani A., Fortin M., Quellet Y., Dhatt G., Bertrand F., "Simple Continuous Pressure Elements for Two- and Three Dimensional Incompressible Flows", *Comput. Meth. Appl. Mech. Eng.*, 62, 1987, pp. 47-69.

Steinbach I., Neises J., "A control volume treatment of finite elements and its application to a solidification problem", *in Numerical Methods in Thermal Problems*, eds. Lewis, R.W. & Durbetaki P., Vol. IX, 1995, pp. 466-473.

Steinbach I., Ein Multi-Phasen-Feld Modell für facettiertes Kristallwachstum, PhD thesis, Technical University Aachen, 2000, http://www.bth.rwth-aachen.de/job/disslist.pl.

Tezduyar T. E., Mittal S., Ray S. E., Shih R., "Incompressible flow computations with stabilized bilinear and linear equal-order-interpolation velocity-pressure elements", *Comput. Meth. Appl. Mech. Eng*., 95, 1992, pp. 221-242.

Zienkiewicz O. C., Onate E., *Finite volumes vs. finite elements. Is there really a choice*?, in *Nonlinear Computation Mechanics, State of the Art*, Wriggers, P. Wagner, W. (eds.), Springer Verlag, Berlin, 1991.